Superconductivity in dense carbon-based materials

Siyu Lu, Hanyu Liu, Ivan I. Naumov, Sheng Meng, Yinwei Li, John S. Tse, Bai Yang, and Russell J. Hemley

Phys. Rev. B **93**, 104509 — Published 8 March 2016

DOI: 10.1103/PhysRevB.93.104509

Superconductivity in dense carbon-based materials

Siyu Lu[a], Hanyu Liu[b,c,1] Ivan I. Naumov[b], Sheng Meng[d], Yinwei Li[e], John S. Tse[c,f], Bai Yang[a,1] and Russell J. Hemley[b,1]

[a]*State Key Laboratory of Supramolecular Structure and Materials, College of Chemistry, Jilin University, Changchun 130012, P. R. China*

[b]*Geophysical Laboratory, Carnegie Institution of Washington, Washington, DC 20015, USA*

[c]*Department of Physics and Engineering Physics, University of Saskatchewan, Saskatoon, Saskatchewan S7N 5E2, Canada*

[d]*Institute of Physics, Chinese Academy of Sciences, Beijing 100190, P. R. China*

[e]*Laboratory for Quantum Design of Functional Materials, School of Physics and Electronic Engineering, Jiangsu Normal University, Xuzhou 221116, P. R. China*

[f]*State Key Laboratory of Superhard Materials, Jilin University, Changchun 130012, P. R. China*

[1]To whom correspondence may be addressed: haliu@carnegiescience.edu, byangchem@jlu.edu.cn, or rhemley@carnegiescience.edu.

Abstract

Guided by a simple strategy in searching of new superconducting materials we predict that high temperature superconductivity can be realized in classes of high-density materials having strong sp^3 chemical bonding and high lattice symmetry. We examine in detail sodalite carbon frameworks doped with simple metals such as Li, Na, and Al. Though such materials share some common features with doped diamond, their doping level is not limited and the density of states at the Fermi level in them can be as high as that in the renowned MgB_2. Together with other factors, this boosts the superconducting temperature (T_c) in the materials investigated to higher levels compared to doped diamond. For example, the superconducting T_c of sodalite-like NaC_6 is predicted to be above 100 K. This phase and a series of other sodalite-based superconductors are predicted to be metastable phases but are dynamically stable. Owing to the rigid carbon framework of these and related dense carbon-materials, these doped sodalite-based structures could be recoverable as potentially useful superconductors.

Introduction

The discovery of superconductivity at 39 K in MgB_2[1] opened up a new perspective in searching for new materials with high critical temperatures T_c. Being well described in terms of the conventional BCS-Eliashberg theory,[2-4] MgB_2 indicates the clear ways how to make similar or even better superconductors. One of the key factors is to have strongly covalent-bonding/antibonding states crossing the Fermi energy E_F. Such states that are similar to σ-electrons in MgB_2 could effectively interact with phonons and therefore lead to high electron-phonon coupling, denoted by the constant λ and thus high T_c. Another important factor is the existence of specific phonons that couple strongly to the covalent states; usually such phonons are bond-stretching vibration modes.

It thus came as no surprise that superconductivity in YbC_6 at 6.5 K[5] and in CaC_6 at 11.5 K[5, 6] was discovered few years after that in MgB_2 – electronically and structurally these materials are similar to MgB_2. They belong to the class of materials called graphite intercalation compounds (GICs) where intercalant (metallic) atoms form layers between the graphene sheets.[7] In GICs, the metal donates some electrons to the graphite antibonding π* band to create superconducting transport.[7] The strength of the electron-phonon coupling on the π* band alone, however, is insufficient to explain the observable T_c's.[8-10] In CaC_6, for example, this contribution is only ~50% to the total value of λ, the other half comes from an intercalant-derived interlayer band as well as from the π*-interlayer interband interactions via out-of-plane carbon vibrations.[8] In GICs, the critical temperature T_c increases with pressure due to the fact that the electron-phonon coupling is sensitive to the distance between the graphene layers.[7] For this reason, MgC_6 is

expected to have a higher T_c than CaC_6; however, attempts to fabricate pure MgC_6 have thus far apparently failed.

Whereas the GIC LiC_6 is not superconducting, it has recently been shown that two-dimensional Li-decorated graphene is a superconductor with a T_c of 5.9 K.[11] In the latter, Li adatoms transfer their electrons to the honeycomb carbon network, thereby shifting the Fermi energy above the Dirac points in the direction of graphene-derived conduction π^* band. Adatoms also strongly modify the phonon spectrum of the system, leading to the relatively high λ of ~0.58. The pairing energy gap opens up on the piece of the π^* Fermi surface around the K-point. The authors propose that superconductivity in Li-decorated graphene is of the same nature as of graphite intercalated compound CaC_6.[11]

At ambient pressure, among all the carbon-based compounds the highest T_c exhibit trivalent alkali-metal doped fullerides A_3C_{60},[12, 13] with $RbCs_2C_{60}$ being an absolute record holder (33 K). All such materials have a high (*fcc*) symmetry and three electrons introduced in the triply degenerate band having t_{1u} symmetry. Noticeably, Cs_3C_{60} has a different (noncubic, base-centered tetragonal) structure than all the other A_3C_{60} systems and is not superconducting at ambient conditions. However, it becomes superconducting under pressure, and its T_c reaches the highest value among all A_3C_{60} compounds (40 K).[12, 13] Importantly, the application of pressure pushes the Cs_3C_{60} system in the direction cubic symmetry; this suggests that the cubic symmetry (or closeness to it) is an essential factor for reaching these relatively high T_c's in trivalent fullerides.

Like layered sp^2–bonded systems, corresponding sp^3 systems can also be turned into superconductors by bringing strong covalent states to the Fermi energy E_F.[14] Thus, when diamond is heavily doped with boron which acts as a charge acceptor, the diamond

becomes a superconductor with a T_c of 4 K.[15] Due to higher symmetry, diamond has more bond stretching phonon branches than does MgB_2: three out of six versus two out of nine in MgB_2.[16] This advantage, however, is more than compensated by two negative factors. First, in going from two to three dimensions the critical phonons become harder reducing the strength of λ,[17] Second, B-doped diamond has a rather small density of states (DOS) at the Fermi level [~0.06 states /eV-atom spin for 2% doping [16]], and, as result, relatively few carriers are available for the superconducting state−this further lowers T_c. Unfortunately, the doping level cannot be increased arbitrarily in the covalent systems , and the introducing of too many dopant atoms can lead to severe mechanical stresses accompanied by misfit dislocations. This problem, however, can be overcome by going from diamond to sp^3 silicon or carbon clathrate structures which allow intercalation [*e.g.*, Refs.[18, 19]]. In doped clathrates, the ratio of intercalated to host network atoms can be as large as 8/46,[20] and the initial Fermi level can be considerably displaced in the valence or conduction bands. For example, into the *n*-doped clathrate Ba_8Si_{46}, E_F is located 1 eV above the conduction band minimum, which is associated solely with Si.[18] Direct calculations of T_c and λ in this system show that its superconductivity is indeed an intrinsic property of the sp^3 network and not directly related to the Ba 5*d* states.[18] In contrast to Ba_8Si_{46}, in *p*-doped FC_{34} E_F is located 0.25 eV below the valence band maximum because an electron is transferred from the carbon network to the guest ion.[19] FC_{34} is predicted to have the highest T_c (77 K) of the silicon and carbon clathrate compounds that have been considered.

Another interesting example is graphane, which is a two-dimensional polymer of carbon and hydrogen, and an sp^3-bonded material like diamond. Due to its reduced

dimensionality and in contrast to diamond, the DOS in graphane exhibits a step function with respect to energy E (as measured from the band edge).[21] As a result, the number of available carriers is sufficient to induce superconductivity even at relatively low doping. Apart from the strong chemical bonds between the carbon atoms and large DOS at E_F, graphane also exhibits a giant Kohn anomaly in optical phonon dispersions.[21] These three factors combined together push the superconducting T_c in graphane above 90 K.[21]

The pursuit of higher temperature superconductors has also led to considering hydrogen-rich materials,[22] including hydrides that may exhibit high T_c behavior analogous to that predicted for metallic hydrogen.[23] Most notably, compressed H_2S was predicted to exhibit very high T_c superconductivity at pressures of 100 GPa.[24] Remarkably, subsequent electrical conductivity and Meissner effect measurements of the H-S system indicate a high T_c reaching 203 K near 200 GPa, the highest critical temperature yet reported for any material.[25] Of particular relevance here is the prediction of very high T_c of 220-235 K for CaH_6 at 150 GPa.[26] This system is in fact an intercalated structure, where the unusual hydrogen sodalite cages contain enclathrated Ca. Similar to doped Si and C clathrates, in CaH_6 the host-derived covalent bands dominate at E_F. It is important that these bands are degenerate at the zone center: the resultant dynamic Jahn-Teller effect enhances λ, leading to high T_c.

The above discussions suggest the following possible simple strategy in the search for new potential high-T_c superconductors. In all of the materials mentioned above, (i) the bonding or antibonding states of covalent nature are expected to intersect the Fermi level and (ii) such states are maximally degenerate at the points of symmetry in the Brillouin zone. Here we show by first-principles calculations that both the conditions can

be met in high symmetry classes of sp^3 bonded carbon framework structures. The properties and relative stabilities of such carbon frameworks are reviewed in Refs.[27, 28] This includes so-called sodalite carbon frameworks which have a *bcc* structure[29] and doped with Li, Na, Al metal atoms. Electron-phonon calculations based on BCS theory predict that these compounds may possess very high superconducting temperatures, *i.e.* above 100 K. Our calculations also suggest that such materials could be synthesized under modest pressures achievable with large volume presses and recoverable as superconductors at pressure.

Results

The total energy and electronic structure of a series of high-symmetry sp^3 bonded carbon framework structures containing different metal atoms were examined. These calculations revealed dynamical stability of sodalite-structured carbides (Fig. 1). We focus on structures with composition XC_6, an important stoichiometry also found in the GICs. We begin with a discussion of NaC_6 as a model system. At zero pressure, its optimized lattice constant is 4.57 Å, with C−C bond of 1.61 Å, which is slightly longer than that the 1.54 Å found in diamond due to the strained square faces (Fig. 1). From the electron localization function one can see that there is strong covalent bonding between the C atoms and only a weak interaction between Na and C atoms. To further understand its electronic properties, we compare the band structures of the empty C_6 cage (Na_0C_6) and NaC_6 (Fig. 2). Without Na, the empty C_6 bcc sodalite framework is a semiconductor with a calculated indirect band gap of 2.48 eV. The top of the valence band is located at the H symmetry point in the first Brillouin zone. This result contrasts with diamond where the valence band maximum is located at Γ. The electronic dispersion curves of

NaC_6 are almost identical to that of C_6 with the Fermi level in NaC_6 shifted up by 3.57 eV due to the additional electrons donated from the Na atoms. Therefore, the doped Na donates electrons to C_6 and the resulting cations only act as spectators and do not significantly alter the band topology of the framework.

When depicted in an extended Brillouin zone, the Fermi surface associated with the lowest conduction band appears as six identical distorted balls "welded" together at H points. In the conventional Brillouin zone, however, this six-piece surface looks like a set of six separate "vases" rather than balls (Fig. 2). One may expect that the nesting features of the Fermi surface leads to strong Kohn anomalies in the phonon spectra. A standard approach to check this is to calculate the real part of the noninteracting susceptibility, Re $\chi_0(q)$.[30, 31] In such a calculation, the peaks or maxima in Re $\chi_0(q)$ indicate the nesting vectors $\mathbf{q}_n$ or positions of possible Kohn anomalies. The calculations show that the highest points of the Re $\chi_0(q)$ curve along the Γ-H, Γ-N and Γ-P directions correspond to $\mathbf{q}$=0.63 $\mathbf{q}_{max}$, $\mathbf{q}$=0.66 $\mathbf{q}_{max}$ and $\mathbf{q}$=0.60 $\mathbf{q}_{max}$, respectively; $\mathbf{q}_{max}$ is the maximal vector along the particular direction (Fig. 3b). These positions correlate well with the positions of Kohn anomalies in the acoustic phonon branches calculated along the corresponding directions (Fig. 3a). As for other directions, H-N and P-N, the predicted positions of Kohn anomalies along them are at $\mathbf{q}$=0.66 $\mathbf{q}_{max}$ and $\mathbf{q}$=0.74 $\mathbf{q}_{max}$, respectively, again in agreement with the calculated phonon spectrum.

The band structure of NaC_6 shows the existence of sharp and flat bands crossing the Fermi energy level. The phonon density of states (PDOS), Eliashberg spectral function $\alpha^2F(\omega)$ and electron-phonon coupling strength $\lambda(\omega)$ for NaC_6 are shown in Fig. 3. The absence of any imaginary phonon modes indicates dynamical stability of the

structure, which we find at both ambient and high pressures. A gap at 300 cm^{-1} (Fig. 3a) separates the phonon spectrum into two regions. The lower frequency branches are associated with the motions of Na and C, whereas the higher frequency branches are mainly associated with C atoms. The combined contribution (43% and 57%, respectively) gives a λ of 2.92.

To illustrate the contributions associated with different phonon modes, circles with radii proportional to the corresponding electron phonon coupling λ_{qj} are plotted in Fig. 3a. It is found that nearly all phonon modes contribute to λ, except acoustic modes at relatively small vectors **q**. Though the latter strongly couple with the electrons at long-wavelengths (**q**→0), they contribute negligibly to the electron-phonon spectral function $\alpha^2F(\omega)$ for small ω because their density of states is proportional to ω^2. The superconductivity is facilitated by the Kohn anomalies realized in the phonon dispersion along different directions in the Brillouin zone (in systems where such anomalies are strong). A large λ also benefits from the high DOS at the Fermi level, which is simply Re $\chi_0(0)$ provided that all the bands that intersect the Fermi level are taken into account.

The superconducting T_c was estimated from the spectral function $\alpha^2F(\omega)$ determined from the numerical solution of the Eliashberg equation[32] using typical choices of the Coulomb pseudopotential μ^* (0.1 to 0.13). The T_c calculated for NaC_6 is 116-127 K at ambient pressure (Fig. 4a), which is an exceptionally high value. We have also examined potential effects of pressure on the superconducting T_c. The calculated λ decreases with increasing pressure, while the average phonon frequency increases (Fig. 4b). Thus, the predicted T_c drops from 116 K at zero pressure to 101 K at 75 GPa, with a

pressure coefficient (*dT/dP*) of 0.2 K/GPa. This change is mainly due to the fact that λ sharply decreases from 2.92 at zero pressure to 1.94 at 25 GPa, and to 1.49 at 75 GPa.

Discussion

According to the Allen-Dynes modified McMillan equation,[33] the critical temperature T_c is determined by two main contributions. T_c is linearly dependent on a characteristic vibrational frequency, the logarithmic average of the phonon spectrum, and exponentially dependent on the electron-phonon coupling parameter λ. Since hydrogen is the lightest element it is expected to possess the highest vibrational frequencies in the compounds. Therefore, the search of high T_c superconductivity has been focused on solid hydrogen and hydrogen-rich materials. However, even a small increase in λ can raise the T_c significantly; this is the case of the sodalite-structured carbide materials investigated here. Remarkably, to the best of our knowledge NaC_6 has the largest predicted λ (2.92) among all the carbon-based materials. For instance, the λ of FC_{34} is predicted to be 0.85.[19]

We now examine the common properties of LiC_6, NaC_6, AlC_6 and SiC_6 that make them all potential high T_c superconductors. As already noted, in the case of NaC_6 the phonons that suffer Kohn anomaly contribute significantly to the Eliashberg function and therefore to λ (Fig. 3a). Though such or even more pronounced anomalies are also seen in the phonon spectra of LiC_6, they are not so evident in the case of AlC_6 and SiC_6 (Fig. S4).[34] So the presence or absence of strong Kohn anomalies is desirable but is not a necessary factor to achieve a relatively high T_c. On the other hand, all of these systems

have a relatively high DOS at the Fermi level. In the case of NaC_6 and AlC_6, for example, $N(E_F)$ = 0.10 states /(eV atom spin); this quantity is close to the 0.12 states /(eV atom spin) found in MgB_2.[3, 4] The fact that the high DOS at E_F does not depend significantly on the doping level or charge transfer from metal elements is related to the ability of flat σ* carbon bands to accommodate up to 6 electrons before the dip in $N(E_F)$ is reached (Fig. 2b).

To confirm this observation, we have performed additional electron phonon coupling calculations on pure sodalite carbon (C_6) structure with additional negative charge (Fig. 3c, d). In C_6 with one additional electron per C_6 unit λ is lower than that found for NaC_6. However, it is still rather large (1.71 versus 2.92), indicating the electron phonon coupling is mainly derived from the metallic carbon-carbon bonds. Moreover, λ is enhanced with increasing the negative charges (up to a critical point >1) as shown in Fig. 3d.

Another common feature of the LiC_6, NaC_6, AlC_6 and SiC_6 systems is that they all have degenerate states close to E_F at some particular points of symmetry. These points are H (LiC_6 and NaC_6), Γ(AlC_6) and P(SiC_6) (Fig. S5).[34] The degenerate states are likely to subject to Jahn–Teller distortion. The John-Teller effect is the coupling between the electronic and nuclear degrees of freedom leading to distortion in the geometric structure and the consequent lifting of orbital degeneracy. If the Jahn-Teller distortion is dynamic, the related vibration as a strong electron-phonon coupling process will lead to superconductivity. The same mechanism has been invoked to explain superconductivity in boron-doped diamond.[15, 35] According to our electronic band structure calculations the latter is also metallic with four bands crossing the Fermi energy, consistent with robust

superconductivity. Our results show that for the sodalite structures, charge transfer between incorporated elements and carbon cage is a key factor in boosting T_c, but only when the transferred charge does not exceed roughly 1 electron. Thus, PC_6, SC_6, ClC_6, SiC_6 and FC_6 have lower critical temperatures than NaC_6, LiC_6 and AlC_6 due to weaker charge transfer (Fig. S2).[34] On the other hand, AlC_6 has larger charge transfer than NaC_6, yet a lower T_c. To further clarify this point, in addition to NaC_6, we examined NaC_{12} (Fig. S6)[34] which is obtained from the former by removing the Na atoms at corner positions in the unit cell. NaC_{12} in this structure is also found to be superconducting with a T_c of 3.8 K ($\lambda = 0.45$). The lower T_c can be explained by the fact that the charge transfer in NaC_{12} is significantly lower than in NaC_6 (0.41 electron/C_6 versus 0.82 electrons/C_6, respectively).

The potentially good superconductors LiC_6, NaC_6, AlC_6 and SiC_6 bear some analogy to the fullerides, GICs, *n*-doped silicon clathrates and MgB_2, which in fact can also be viewed as an intercalated material with parallels to graphite. In the case of the aforementioned sodalite systems, metallic elements act as donors with respect to carbon, similar to intercalants in fullerides, graphite or Mg relative to B. The degree of doping , however, is different. Whereas Li and Na donate almost all valence (*s*) electrons to carbon [similar to alkali metals in fullerides or Mg in MgB_2[4]], Al and Si only partially transfer their valence electrons, similar to GICs.[7, 9, 10, 33] Ba-doped silicon clathrates[20] and Ca- and Yb-doped graphene.[36, 37] As a result, no dopant-derived bands form near the Fermi energy in LiC_6 and NaC_6, but such bands do form in AlC_6 and SiC_6. They cross the Fermi level and strongly hybridize with the host-atom (C) states like the analogous bands in GICs, silicon clathrates or doped graphene. As pointed out in previous studies, such

hybridization leads to a strong enhancement of the electron-phonon interaction and contributes to superconductivity.[10, 20, 33, 35, 36] In the case of GICs, for example, electrons associated with the intercalant-derived bands interact strongly with carbon atom vibrations perpendicular and metal vibrations parallel to graphite layers.[9, 10, 33] A similar effect is possible in AlC_6 and SiC_6, where the sodalite-carbon network has some parallels to the graphite structure, in the sense of having ideal hexagons and squares sharing common sides. In contrast to GICs and other similar systems just discussed above, there are no occupied metal-derived bands in MgB_2, instead the B-derived bonding σ band is only partly filled and the hole-like σ states strongly interact with the bond-stretching phonons, providing the necessary conditions to realize high-temperature superconductivity.[3, 4] Similar to fullerides and MgB_2, in LiC_6 and NaC_6 the antibonding C-derived σ* states are partly occupied and strongly interact with a number of different phonons, especially with those exhibiting a Kohn anomaly.

Our results indicate that the existence of degenerate states (especially those triply degenerate) at high symmetry points in the Brillouin zone should be considered as a promoting factor in achieving high T_c. To strengthen this point, we also investigated the effect of distortions on the electronic properties of NaC_6. (Fig. S7)[34] We found that in the tetragonal structure with a=c=4.57 A and c=4.67 A, the electron-phonon coupling constant λ drops to 2.07 compared to 2.92 in initial cubic structure The corresponding calculated T_c is 82 K versus 116 K in the cubic phase. In the context of the role of cubic symmetry, our XC_6 systems are parallel to *fcc* alkali-doped fullerides, where the t_{1u} band is very similar to the C-derived σ* band in the systems studied. As discussed above, the

cubic symmetry is crucial for realizing superconductivity with enhanced T_c's in A_3C_{60} systems.[12, 13]

The triple degeneracy in the sodalite framework structure is easily realized, even if the degenerate bands are 1*s*-derived, as is the case for CaH_6.[26] Indeed, any atom occupying Wyckoff positions 12*d* in the *Im-3m* space group (*e.g.,* C or H for NaC_6 and CaH_6) will inevitably lead at least to one of the four possible triply degenerate Bloch states at the H point (H_4^+, H_4^-, H_5^+ and H_5^-). At the same time, all atoms whose orbitals transform according to the irreducible representations A_1, B_1 and E can induce the Bloch states Γ_4^-, Γ_5^+ which are triply degenerate at Γ.[38] This common symmetry, in addition to the low-Z character of the atomic framework, is an important factor underlying the high T_c calculated at the same level of theory for the two materials.

We now comment on the stability of these structures. The XC_6 phases examined have higher enthalpy than the elemental assemblage of diamond plus and solid alkali metal (Fig. S3).[34] The higher energy arises from strained sp^3 bonds of the sodalite cage. The dynamical stability of NaC_6 and other sodalite-based carbon structures (XC_6, X=H, Li, N, O, F, Al, Si, P, S and Cl) under ambient pressures and the strong covalently bonded carbon structures indicate they should possess large kinetic energy barriers with respect to transformations to lower density forms. Thus, by analogy to diamond and other sp^3 bonded carbon structures that are formed under pressure, these materials may be recoverable to ambient conditions (Fig. S3 and Fig. S4).[34]

Conclusions

By following some simple criteria for the existence of phonon-mediated high-T_c superconductors we discovered a new class of materials that potentially can have T_c of the order 100K and higher−doped sodalite-structured carbide compounds. These materials are characterized by strong sp^3 bonding, high crystal symmetry and large number of electrons transferred from a dopant to the host lattice. All the mentioned features contribute to their strong electron-phonon couplings in ($\lambda \sim 1$). Among all the studied XC_6 systems, NaC_6 has the highest predicted T_c at ambient pressure (above 100 K). This is followed by AlC_6 and LiC_6, where T_c can reach 85-95 K. As rigid sp^3 bonded structures, carbon sodalite networks may be kinetically stable at ambient pressure. Dense superconductive states, such as those reported here, may be favored in other mixtures of elemental metals plus carbon and/or upon compression.

Computational details

Our calculations have been mainly performed for XC_6 compounds in cubic *Im*-3*m* structure (2 f.u./unit cell), where X atoms organize a Bravais *bcc* lattice and carbon atoms form squared C_4 and hexagonal C_6 rings that share some common sides (Fig. 1a). These C_4 and C_6 rings are interlinked in such a way that they form a sodalite framework with an X atom enclathrated at the center of each cage consisting of 24 atoms. Each carbon atom is sp^3 bonded to four carbon atoms with C-C-C angles of 90° and 120°. The optimized lattice parameters were found using density functional theory within the Perdew-Burke-Ernzerhof (PBE)[39] generalized gradient approximation as implemented in the Quantum-ESPRESSO package.[40] Phonon dispersion and electron-phonon coupling calculations were performed with density functional perturbation theory using the Quantum-ESPRESSO package. Ultrasoft pseudopotentials for Na and C were employed with a

kinetic energy cutoff of 80 Ry. A *q*-mesh of 4×4×4 in the first Brillouin zone was used in the electron-phonon coupling calculations. A *k*-mesh of 16×16×16 were adopted to ensure *k*-points sampling convergence with a Gaussian width of 0.04 Ry in order to approximate the zero-width limit in the calculations of λ. The real part susceptibility of noninteracting electrons Re $\chi_0(q)$ was calculated by using the highly precise analytic tetrahedron method. In order to reach high precision in the Re $\chi_0(q)$, the irreducible part of the Brillouin zone was divided into 16,000 tetrahedra. Additional computational details can be found in the Supporting Information.

Acknowledgements

This work was supported by the National Science Foundation of China (51373065, 91123031 and 21221063), the National Basic Research Program of China (2012CB933800), and Specialized Research Fund for the Doctoral Program of Higher Education (20130061130010). Part of the calculations has been performed by the use of computing resources provided by WestGrid and Compute Canada. J.T. and H.L. acknowledge the National Science Foundation of China (11474126) and support from the University of Saskatchewan research computing group and the use of the HPC resources (Plato machine). Work at Carnegie was supported by EFree, an Energy Frontier Research Center funded by the DOE, Office of Science, Basic Energy Sciences under Award No. DE-SC-0001057 (salary support for H.L). The infrastructure and facilities used at Carnegie were supported by NNSA Grant No. DE-NA-0002006, CDAC. This work is also a contribution to the Deep Carbon Observatory.

References

[1] J. Nagamatsu, N. Nakagawa, T. Muranaka, Y. Zenitani, and J. Akimitsu, Nature **410**, 63 (2001).

[2] J. M. An and C. J. Pickard, Phys. Rev. Lett. **86**, 4366 (2001).

[3] H. J. Choi, D. Roundy, H. Sun, M. L. Cohen, and S. G. Louie, Nature **418**, 758 (2002).

[4] J. Kortus, I. I. Mazin, K. D. Belashchenko, V. P. Antropov, and L. L. Boyer, Phys. Rev. Lett. **86**, 4656 (2001).

[5] T. E. Weller, M. Ellerby, S. S. Saxena, R. P. Smith, and N. T. Skipper, Nat. Phys. **1**, 39 (2005).

[6] N. Emery, C. Hérold, M. d'Asturo, V. Garcia, C. Bellin, J. F. Marêché, P. Lagrange, and G. Loupias, Phys. Rev. Lett. **95**, 087003 (2005).

[7] R. P. Smith, T. E. Weller, C. A. Howard, M. P. M. Dean, K. C. Rahnejat, S. S. Saxena, and M. Ellerby, Physica C **514**, 50 (2015).

[8] S. L. Yang, J. A. Sobota, C. A. Howard, C. J. Pickard, M. Hashimoto, D. H. Lu, S. K. Mo, P. S. Kirchmann, and Z. X. Shen, Nat. Commun. **5**, 3493 (2014).

[9] G. Csányi, P. B. Littlewood, A. H. Nevidomskyy, C. J. Pickard, and B. D. Simons, Nat. Phys. **1**, 42 (2005).

[10] M. Calandra and F. Mauri, Phys. Rev. Lett. **95**, 237002 (2005).

[11] B. M. Ludbrook, et al., Proc. Natl. Acad. Sci. USA **112**, 11795 (2015).

[12] O. Gunnarsson, Rev. Mod. Phys. **69**, 575 (1997).

[13] Y. Iwasa and T. Takenobu, J. Phys.: Condens. Matter **15**, R495 (2003).

[14] X. Blase, E. Bustarret, C. Chapelier, T. Klein, and C. Marcenat, Nat. Mater. **8**, 375 (2009).

[15] E. A. Ekimov, V. A. Sidorov, E. D. Bauer, N. N. Mel'Nik, N. J. Curro, J. D. Thompson, and S. M. Stishov, Nature **428**, 542 (2004).

[16] K. W. Lee and W. E. Pickett, Phys. Rev. Lett. **93**, 237003 (2004).

[17] L. Boeri, J. Kortus, and O. K. Anderson, Phys. Rev. Lett. **93**, 237002 (2004).

[18] D. Connétable, et al., Phys. Rev. Lett. **91**, 247001 (2003).

[19] F. Zipoli, M. Bernasconi, and G. Benedek, Phys. Rev. B **74**, 205408 (2006).

[20] H. Kawaji, H. Horie, S. Yamanaka, and M. Ishikawa, Phys. Rev. Lett. **74**, 1427 (1995).

[21] G. Savini, A. C. Ferrari, and F. Guistino, Phys. Rev. Lett. **105**, 037002 (2010).

[22] N. Ashcroft, Phys. Rev. Lett. **92**, 187002 (2004).

[23] N. W. Ashcroft, Phys. Rev. Lett. **21**, 1748 (1968).

[24] Y. Li, J. Hao, H. Liu, Y. Li, and Y. Ma, J. Chem. Phys **140**, 174712 (2014).

[25] A. P. Drozdov, M. I. Eremets, I. A. Troyan, V. Ksenofontov, and S. I. Shylin, Nature **525**, 73 (2015).

[26] H. Wang, S. T. John, K. Tanaka, T. Iitaka, and Y. Ma, Proc. Natl. Acad. Sci. USA **109**, 6463 (2012).

[27] N. Rey, A. Munoz, P. Rodriguez-Hernandez, and A. San Miguel, J. Phys.: Condens. Matter **20**, 215218 (2008).

[28] T. Zeng, R. Hoffmann, R. Nesper, N. Ashcroft, T. A. Strobel, and D. M. Proserpio, J. Am. Chem. Soc. **137**, 12639 (2015).

[29] F. J. Ribeiro, P. Tangney, S. G. Louie, and M. L. Cohen, Phys. Rev. B **74**, 172101 (2006).

[30] A. Landa, J. Klepeis, P. Söderlind, I. Naumov, O. Velikokhatnyi, L. Vitos, and A. Ruban, J. Phys.: Condens. Matter **18**, 5079 (2006).
[31] M. D. Johannes and I. I. Mazin, Phys. Rev. B **77**, 165135 (2008).
[32] G. M. Eliashberg, Sov. Phys. JETP. **11**, 696 (1960).
[33] P. B. Allen and R. C. Dynes, Phys. Rev. B **12**, 905 (1975).
[34] See supplemental material at [URL will be inserted by publisher] for [Details on the calculations, Fig. S2 shows the superconductivity, Fig. S3 shows the Enthalpy difference, Fig. S4 shows the phonon spectra, Fig. S5 shows the calculated band structures and Fig. S6 shows the crystal structures of NaC_6 and NaC_{12}].
[35] Y. Ma, J. S. Tse, T. Cui, D. Klug, L. Zhang, Y. Xie, Y. Niu, and G. Zou, Phys. Rev. B **72**, 014306 (2005).
[36] M. Calandra and F. Mauri, Phys. Rev. B **76**, 161406(R) (2007).
[37] C. Hwang, et al., Phys. Rev. B **90**, 115417 (2014).
[38] M. I. Aroyo, J. M. Perez-Mato, C. Capillas, E. Kroumova, S. Ivantchev, G. Madariaga, A. Kirov, and H. Wondratschek, Z. Krist. **221**, 15 (2006).
[39] J. P. Perdew, K. Burke, and M. Ernzerhof, Phys. Rev. Lett. **77**, 3865 (1996).
[40] P. Giannozzi, S. Baroni, N. Bonini, M. Calandra, R. Car, C. Cavazzoni, and D. Ceresoli, J. Phys.: Condens. Matter **21**, 395502 (2009).

Figure Captions

Figure 1. Crystal structures of (a) GIC-XC_6, (b) sodalite-type XC_6 (b), and (c) sodalite-type XC_{12}.

Figure 2. Electronic band structures. (a) Band structure of C_6. (b) Band structure of NaC_6. The horizontal dotted lines indicate the Fermi level. The red and blue bands are crossing the Fermi level. Insert shows the Fermi surface corresponding to the red and blue bands along H-N.

Figure 3. Phonon properties and Eliashberg spectral function. (a) Phonon dispersions, projected PDOS, Eliashberg spectral function $\alpha^2F(\omega)/\omega$ and electron-phonon coupling integration of $\lambda(\omega)$ of NaC_6. (b) Re $\chi_0(q)$ along the Γ-H, Γ-N and Γ-P lines of the Brillouin zone in NaC_6. Only contributions from the lowest conduction band are taken into account because they define the shape of Re $\chi_0(q)$. The red arrows indicate the positions of the peaks that correlate with the positions of the Kohn anomalies in the phonon dispersions (panel *a*). (c) Phonon dispersions, phonon DOS, Eliashberg spectral function $\alpha^2F(\omega)/\omega$ and electron-phonon coupling integration of $\lambda(\omega)$ of C_6 with one additional negative charge. (d) The calculated superconducting temperature T_c and the electron phonon coupling parameter as a function of pressure. The size of red circles in panels (a) and (c) is proportional to λ_{qj} which is given by formula (4) in Supporting Information.

Figure 4. Predicted superconductivity in XC_6. (a) T_c of NaC_6 at ambient pressure. (b) Superconductivity gap of NaC_6**.** (b) T_c as a function of pressure. The coupling parameters, the average phonon frequencies ω_{log} and superconducting temperatures of NaC_6 are shown as a function of pressure.

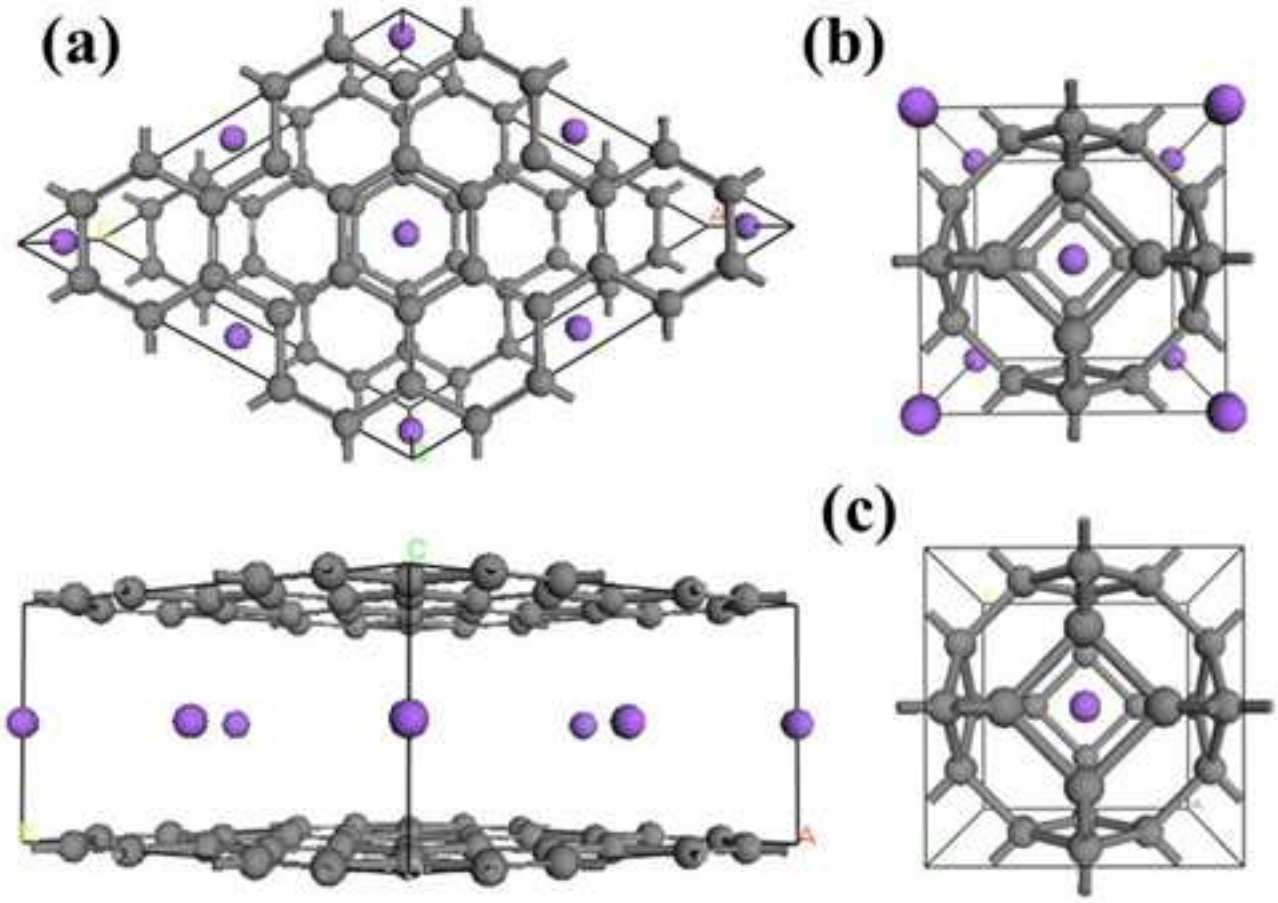

Figure 1 BL12862 11JAN2016

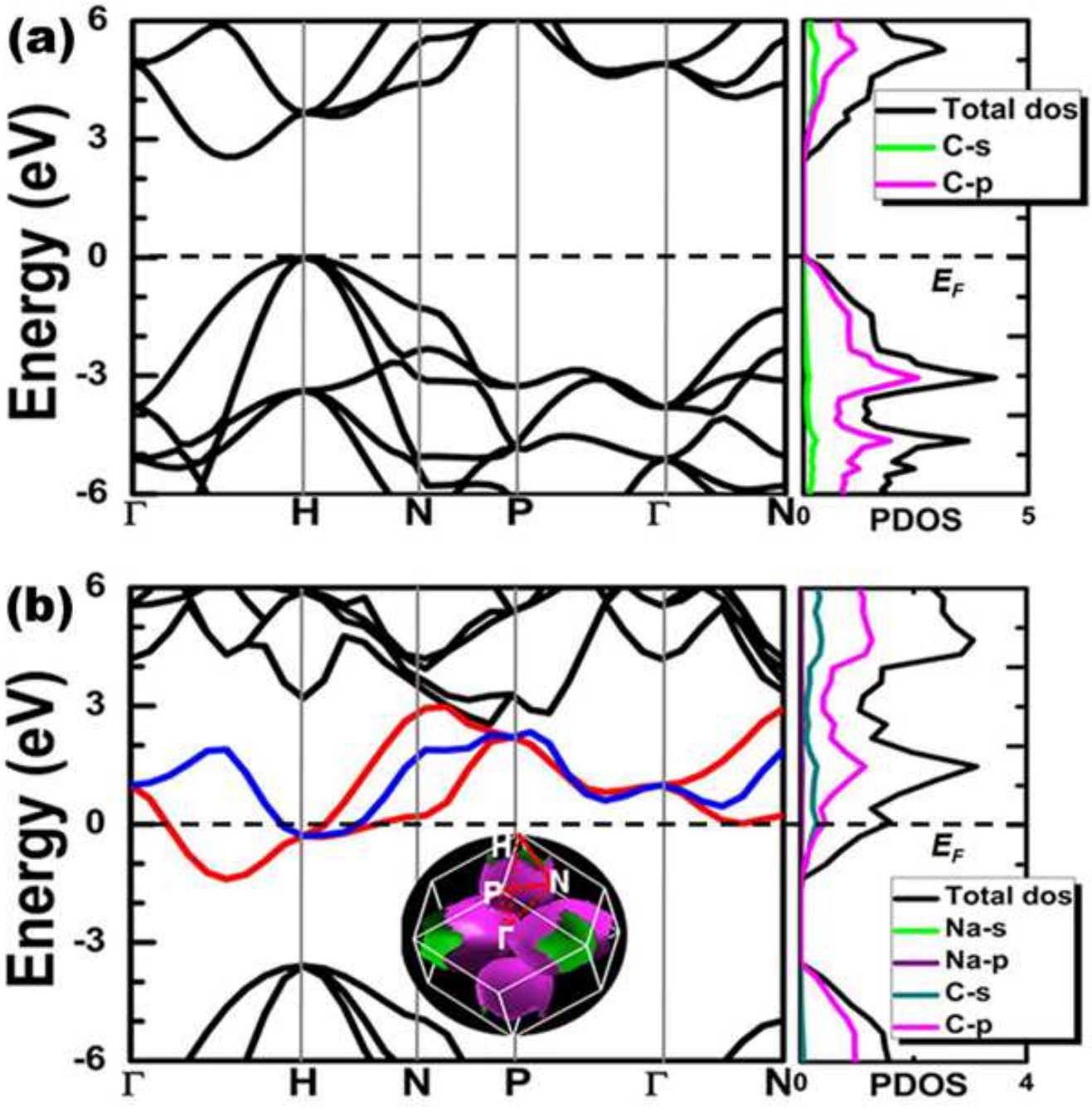

Figure 2 BL12862 11JAN2016

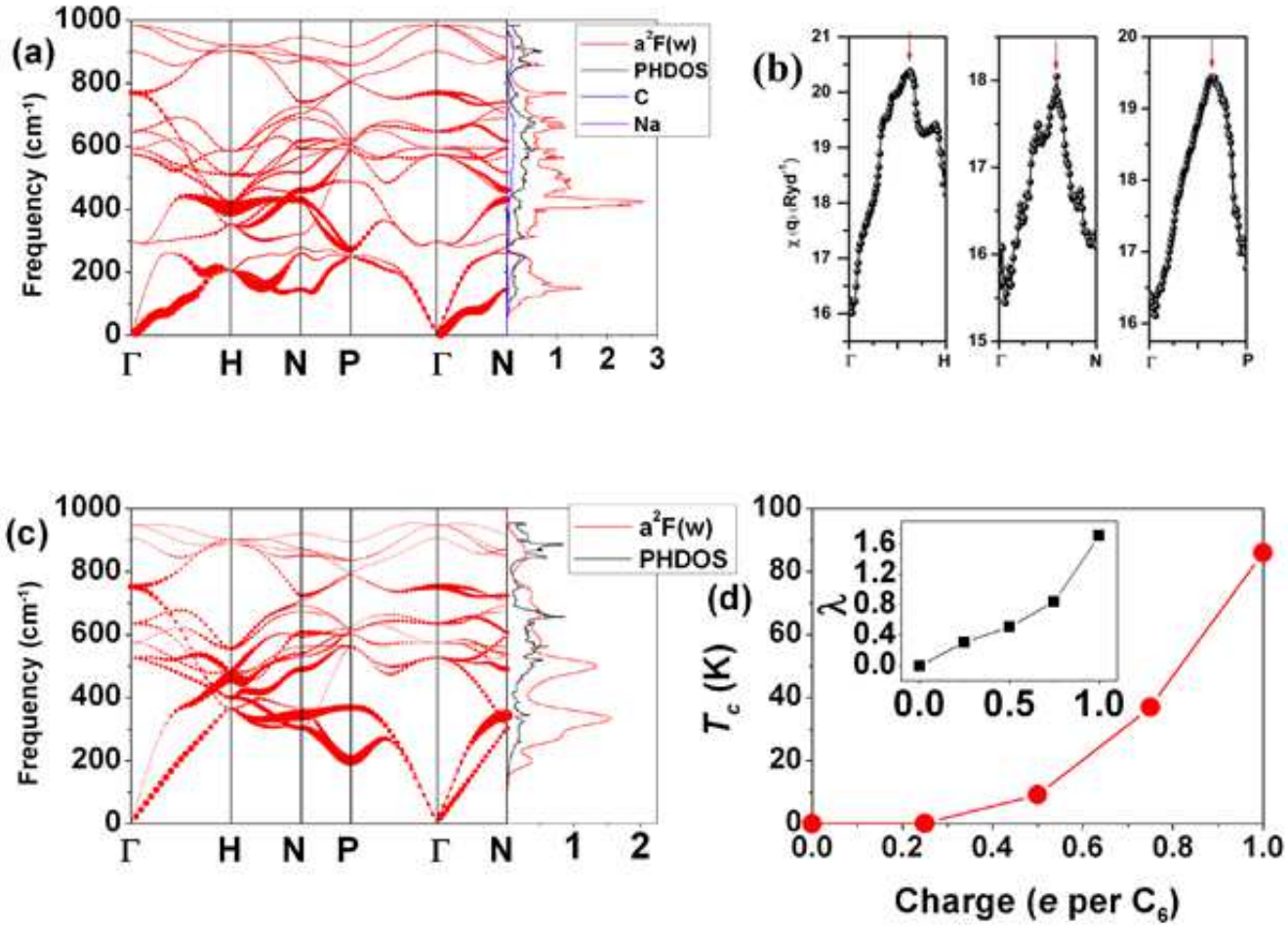

Figure 3 BL12862 11JAN2016

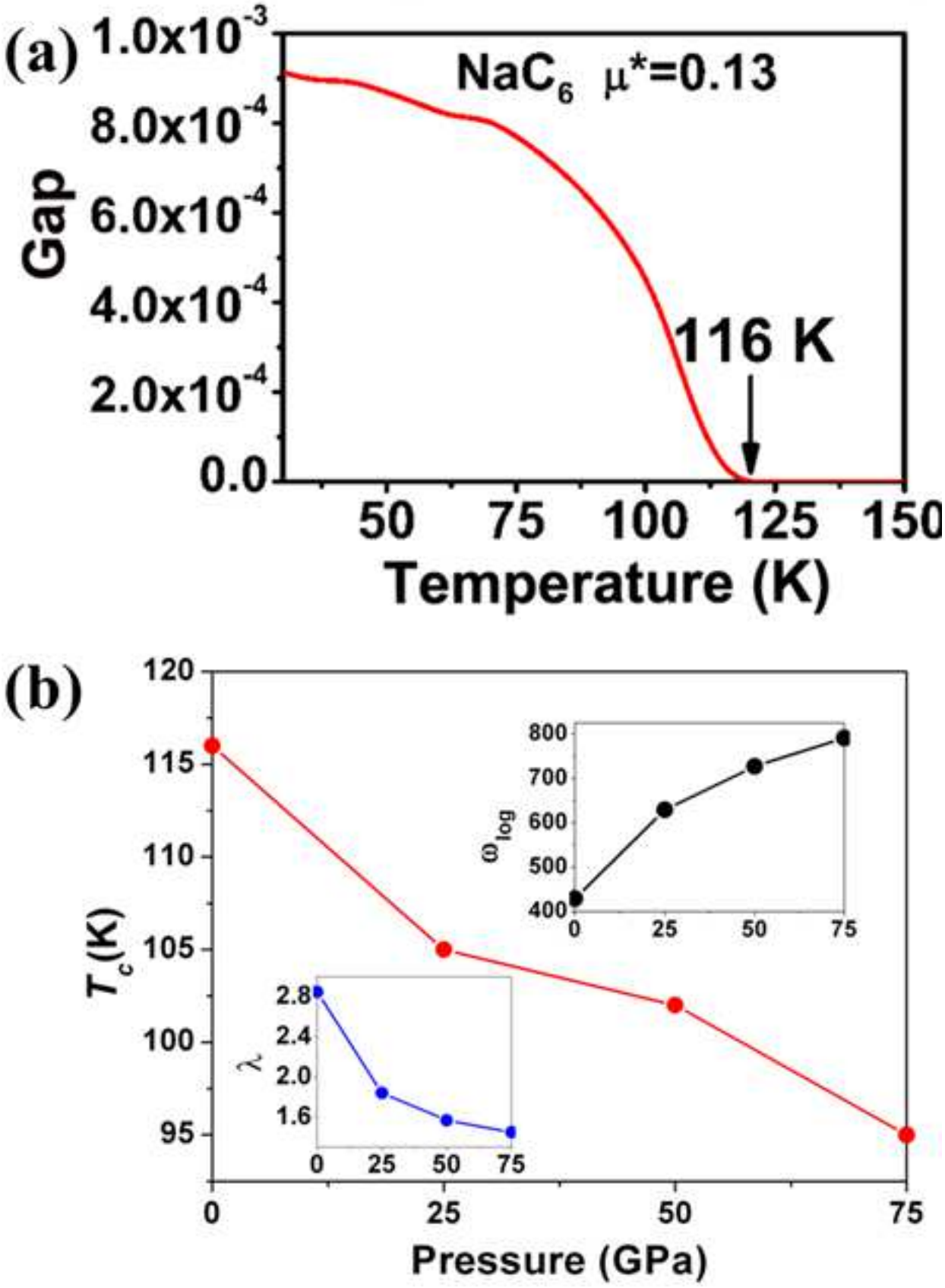

Figure 4 BL12862 11JAN2016